

## Galectins Bind to the Multivalent Glycoprotein Asialofetuin with Enhanced Affinities and a Gradient of Decreasing Binding Constants<sup>†</sup>

Tarun K. Dam,<sup>‡</sup> Hans-J. Gabius,<sup>§</sup> Sabine André,<sup>§</sup> Herbert Kaltner,<sup>§</sup> Martin Lensch,<sup>§</sup> and C. Fred Brewer<sup>\*,‡</sup>

Departments of Molecular Pharmacology, and Microbiology and Immunology, Albert Einstein College of Medicine, Bronx, New York 10461, and Institut für Physiologische Chemie, Tierärztliche Fakultät, Ludwig-Maximilians Universität München, 80539 München, Germany

Received June 14, 2005; Revised Manuscript Received July 15, 2005

**ABSTRACT:** Our previous isothermal titration microcalorimetry (ITC) studies of the binding of synthetic multivalent carbohydrates to the Man/Glc-specific lectins concanavalin A (ConA) and *Dioclea grandiflora* lectin (DGL) showed negative binding cooperativity that was due to the carbohydrate ligands and not the proteins [Dam, T. K., et al. (2002) *Biochemistry* 41, 1351–1358]. The negative cooperativity was associated with the decreasing functional valence of the carbohydrates upon progressive binding of their epitopes. The present study also shows negative cooperativity in the ITC binding data of asialofetuin (ASF), a glycoprotein that possesses nine LacNAc epitopes, to galectin-1, -2, -3, -4, -5, and -7, and truncated, monomer versions of galectin-3 and -5, which are members of a family of animal lectins. Although the observed  $K_a$  values for binding of ASF to the galectins and two truncated forms are only 50–80-fold greater than that of LacNAc, analysis of the data in terms of the relationship between the observed macroscopic free energy of binding and the decreasing microscopic free energies of binding of the epitopes shows that the first LacNAc epitope of ASF binds with approximately 6000-fold higher affinity than the last epitope. Thus, the microscopic binding constants of the galectins for the first epitope(s) of ASF are in the nanomolar range, with a gradient of decreasing binding constants of the remaining epitopes. The results indicate that the above galectins bind with fractional, high affinities to multivalent glycoproteins such as ASF, independent of the quaternary structures of the galectins. These findings have important implications for the binding of galectins to multivalent carbohydrate receptors.

The glycan chains of many naturally occurring glycoproteins often possess multiple copies of the same carbohydrate epitope (cf. 1). One effect of this carbohydrate multivalency is to increase the affinity (avidity) of a glycoprotein for specific carbohydrate binding receptors, including lectins (2, 3). The multivalency of glycoproteins can be of two types, or combinations of the two. First, glycoproteins often possess asparagine (N<sup>1</sup>)- or serine/threonine (O)-linked branched chain carbohydrates that are themselves multivalent (4), or multiple glycan chains at different sites that confer multivalency to the glycoprotein (5).

Both types of multivalency are present in the glycoprotein asialofetuin (ASF). ASF possesses three N-linked triantennary chains with nine terminal LacNAc residues that are available for binding to LacNAc-specific lectins, including galectin-1 (5, 6). Galectin-1 is a member of the  $\beta$ -Gal-specific

galectin family of animal lectins of which there are currently 15 members. Their biological properties include the regulation of cell adhesion and cell growth (cf. 7). Since ASF is a naturally occurring multivalent glycoprotein that induces homotypic aggregation of tumor cells in the presence of certain galectins (8), it is important to understand the thermodynamics and mechanisms of binding of ASF to galectins.

Isothermal titration microcalorimetry (ITC) has been shown to be a powerful technique for investigating the thermodynamics of binding of multivalent carbohydrates to lectins (9). ITC data for the binding of di-, tri-, and tetravalent carbohydrate analogues of Man to the Man/Glc-specific lectins concanavalin A (ConA) and *Dioclea grandiflora* lectin (DGL) (10) showed that increases in the  $K_a$  values of the multivalent analogues were due to greater positive entropy ( $T\Delta S$ ) contributions. The ITC data for the analogues were also subjected to Hill plot analysis that detects cooperativity in the binding of ligands to macromolecules (cf. 11, 12). The results demonstrated curvilinear Hill plots consistent with increasing negative cooperativity for binding of the di-, tri-, and tetravalent carbohydrates to both lectins. The corresponding monovalent carbohydrate, on the other hand, showed no cooperativity effects (13). Thus, the negative cooperativity was associated with the multivalent carbohydrates and not the lectins, and posited to be due to the decreasing functional valence of the carbohydrates upon progressive binding of the multiple carbohydrate epitopes.

<sup>†</sup> This work was supported by Grant CA-16054 from the National Cancer Institute, Department of Health, Education and Welfare, and Core Grant P30 CA-13330 from the same agency (C.F.B.) and a grant from the Mizutani Foundation for Glycoscience, Tokyo, Japan (H.-J.G.).

<sup>\*</sup> To whom correspondence should be addressed. Telephone: (718) 430-2227. Fax: (718) 430-8922. E-mail: brewer@aeom.yu.edu.

<sup>‡</sup> Albert Einstein College of Medicine.

<sup>§</sup> Ludwig-Maximilians Universität München.

<sup>1</sup> Abbreviations: N, asparagine; O, serine/threonine; ASF, asialofetuin; ITC, isothermal titration calorimetry; ConA, concanavalin A; DGL, *Dioclea grandiflora* lectin; CRD, carbohydrate recognition domain; LacNAc, N-acetyl-D-lactosamine.

In the study presented here, ITC has been used to investigate the thermodynamics of binding of ASF to galectin-1, -2, -3, -4, -5, and -7, which are members of the galectin family of animal lectins (14), as well as to truncated monomeric galectin-3 and -5 which consist of only the carbohydrate recognition domain (CRD) of each protein. The structures of these galectins fall into three main types: the proto type (galectin-1, -2, -5, and -7) that exists as a monomer or homodimer; the chimera type (galectin-3) that contains a non-lectin N-terminal short sequence segment followed by 8–12 collagen-like repeats of nine amino acids connected to the C-terminal CRD; and tandem repeat type (galectin-4, -6, -8, -9, and -12) which is composed of two distinct CRDs in a single polypeptide chain connected by a linker peptide (15–19). The specificity of these galectins has been generally shown to be toward LacNAc residues, with higher affinities for longer chain glycans (20, 21).

The present ITC data show 50–80-fold higher affinities of ASF for human galectin-1, -2, -3, -4, and -7, rat galectin-5 (for which there is no human homologue), and truncated galectin-3 and -5, relative to LacNAc. In addition, Hill plots of the raw ITC data show increasing negative cooperativity for ASF binding to the all of the galectins, including truncated galectin-3 and -5. These results have important implications for the mechanisms of binding of galectins to cellular glycoprotein receptors.

## MATERIALS AND METHODS

**Materials.** Bovine fetuin was obtained from Sigma Chemical Co. ASF was prepared as previously described (5). *N*-Acetyllactosamine (type II) was obtained from Sigma Chemical Co. All other reagents were of analytical grade.

**Recombinant Galectins.** Production of recombinant human galectin-1, -2, -3, -4, and -7 and rat galectin-5 used either pQE-60 (Qiagen, Hilden, Germany) or pET12a (Novagen, Darmstadt, Germany) system followed by affinity chromatography on lactosylated Sepharose 4B, obtained by activation with divinylsulfone (22–24). Total RNA from the acute myelogenous leukemia line KG-1 was starting material for cloning of human galectin-4 cDNA using the sense primer 5'-CGTACGCATATGGCCTATGTCCCGCACC-3' with an internal *Nde*I restriction site (underlined) and the antisense primer 5'-GCTAGGTCGACTTAGATCTGGACATAGG-3' with an internal *Sal*I restriction site (underlined) in PCR amplification. Following a propagation stage in the pET-Blue-1 AccepTor vector (Novagen, Bad Soden, Germany), recombinant expression was accomplished in the pET-12a/*Escherichia coli* strain BL21(DE3)pLysS and TB medium (Roth, Karlsruhe, Germany) at 30 °C with a final IPTG concentration of 75  $\mu$ M with optimal yields reaching 6–10 mg/L. Quality controls were routinely performed by one- and two-dimensional gel electrophoreses, gel filtration, hemagglutination, and solid-phase assays to ascertain homogeneity, quaternary structure, and activity (24, 25). Proteolytically truncated human galectin-3 was prepared by collagenase digestion of the N-terminal part as described for murine galectin-3 (26). The short N-terminal tail of 14 amino acids of rat galectin-5 was removed on the cDNA level by RT-PCR amplification of the full-length sequence using modified primer sets with 5'-CGTACGCCATGGTACCTTTCTTCACCAGC-3' (sense) and 5'-CGCTAGAAGCTTAGGTCTCCACGTGTG-3' (antisense) to eliminate the first

exon. The pQE60/*E. coli* strain M15 system (Qiagen) and TB medium at 37 °C with a final IPTG concentration of 150  $\mu$ M was used for expression, with yields reaching 1.5 mg/L. The purified CRDs moved as single bands on SDS–PAGE.

Subunit lectin concentrations were determined spectrophotometrically at 280 nm using specific extinction coefficients of the proteins (E1%1cm). A value of 5.4 (E1%1cm) was used for galectin-1 and -2, 6.1 (E1%1cm) for galectin-3, 5.5 (E1%1cm) for truncated galectin-3 CRD, 6.4 (E1%1cm) for galectin-4, 5.7 (E1%1cm) for galectin-5, 5.4 (E1%1cm) for truncated galectin-5 CRD, and 5.5 (E1%1cm) for galectin-7 as determined from ITC experiments described previously (26). Molecular masses of the galectin subunits were determined by MALDI and electrospray ionization mass spectrometry and were found to be 14 500 Da for galectin-1, 14 600 Da for galectin-2, 29 000 Da for galectin-3, 14 500 Da for galectin-3 CRD, 36 000 Da for galectin-4, 16 000 Da for galectin-5, 14 500 Da for galectin-5 CRD, and 14 600 Da for galectin-7. The carbohydrate concentration was measured by the phenol/sulfuric acid method (27, 28).

**Isothermal Titration Microcalorimetry.** ITC experiments were performed using a VP-ITC instrument from Microcal, Inc. (Northampton, MA). Injections of 4  $\mu$ L of a carbohydrate solution were added from a computer-controlled microsyringe at an interval of 4 min into the sample solution of lectin (cell volume = 1.43 mL) with stirring at 310 rpm. An example of an ITC experiment is shown in Figure 1 for ASF and human galectin-3 at 27 °C. Control experiments were performed by making identical injections of ASF into a cell containing buffer. The concentration range of the galectins was 15–90  $\mu$ M and for ASF 0.14–0.63 mM. Titrations were carried out at pH 7.2 using 20 mM PBS buffer. The experimental data were fitted to a theoretical titration curve using software supplied by Microcal, with  $\Delta H$  (binding enthalpy in kilocalories per mole),  $K_a$  (association constant), and  $n$  (number of binding sites per monomer) as adjustable parameters. The quantity  $c = K_a M_t(0)$ , where  $M_t(0)$  is the initial macromolecule concentration, is important in titration microcalorimetry (29). All experiments were performed with  $c$  values between 1 and 200. The instrument was calibrated using the calibration kit containing ribonuclease A (RNase A) and cytidine 2'-monophosphate (2'-CMP) supplied by the manufacturer. Thermodynamic parameters were calculated from the Gibbs free energy equation  $\Delta G = \Delta H - T\Delta S = -RT \ln K_a$ , where  $\Delta G$ ,  $\Delta H$ , and  $\Delta S$  are the changes in free energy, enthalpy, and entropy of binding, respectively.  $T$  is the absolute temperature, and  $R = 1.98 \text{ cal mol}^{-1} \text{ K}^{-1}$ .

**Hill Plot ITC Data Analysis.** The total concentration of ligand  $X_t(i)$  as well as lectin  $M_t(i)$  after the  $i$ th injection and the heat evolved on the  $i$ th injection,  $Q(i)$ , are readily available from the ITC raw data file after each experiment. The concentration correction is automatically carried out with Origin.

The concentration of bound ligand  $X_b(i)$  after the  $i$ th injection is

$$X_b(i) = [Q(i)/(\Delta H V_o)] + X_b(i-1) \quad (1)$$

where  $Q(i)$  (microcalories) is the heat evolved on the  $i$ th injection,  $\Delta H$  (calories per mole) the enthalpy change,  $V_o$  (milliliters) the active cell volume, and  $X_b$  (millimolar) the

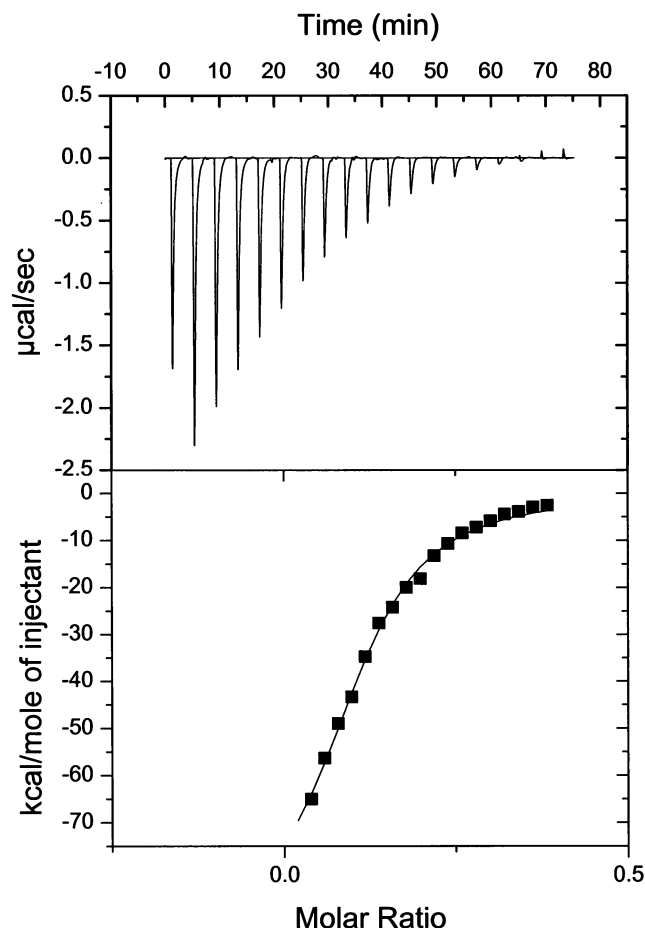


FIGURE 1: ITC binding profile of human galectin-3 (34  $\mu$ M) with ASF (330  $\mu$ M) at 27  $^{\circ}$ C. The top panel shows data obtained for automatic injections, 4  $\mu$ L each, of ASF; the bottom panel shows the integrated curve showing experimental points (■) and the best fit (—).

concentration of bound ligand.  $X_b$  is equal to  $M_b$ , the concentration of bound protein, and in this study of multivalent ligands, the more general expression is  $M_b = (X_b) \times$  (functional valency of ligand). The concentration of free ligand ( $X_f$ ) after the  $i$ th injection was determined as follows

$$X_f(i) = X_t(i) - X_b(i) \quad (2)$$

Hill plots were constructed by plotting  $\log\{Y(i)/[1 - Y(i)]\}$  versus  $\log[X_f(i)]$ , where  $Y(i) = [X_b(i)] \times$  (functional valency of ligand)/ $M_t(i)$ , which is a modified version of the Hill plot (cf. 12) that takes into account the functional valency of the ligand. The functional valency of ASF in binding the galectins was obtained from the  $n$  values in Table 1 and is listed in the figure legend for the Hill plots.

A program was created using Microsoft Excel for construction of Hill plots. Work sheet data of total ligand as well as total lectin concentration and the amount of heat evolved were copied from the ITC raw data file and pasted on the appropriate columns of the program. After calculation, the program shows a Hill plot. Delta Graph was then used for further analysis of the plot.

The validity of the information obtained from the Hill plot  $\{\log[Y/(1 - Y)] \text{ versus } \log(X_f)\}$  was tested by directly fitting the binding data of monovalent LacNAc to the Hill equation. The Hill slope was found to be the same by direct fitting or

plotting the Hill equation data. Similar attempts at direct fitting of the ITC data for ASF failed since the Hill  $n$  values change throughout the binding process.

## RESULTS AND DISCUSSION

Previous studies have shown that galectin-1 and -3 precipitate with ASF under certain stoichiometric conditions (cf. 30). However, using relatively low concentrations of both ASF and the galectins in this study prevented their precipitation during the ITC experiments.

**ITC  $K_a$  Values for Binding of ASF to Galectin-1, -2, -3, -4, -5, and -7.** The ITC-derived  $K_a$  values,  $K(\text{obs})$ , for binding of ASF to galectin-1, -2, -3, -4, -5, and -7 are between 50–80-fold greater than that of the corresponding  $K_a$  values for LacNAc (Table 1). The  $K_a$  values for the truncated galectin-3 and -5 are also similar to those of the corresponding intact galectins (Table 1). Since galectin-1 and -7 have been shown by sedimentation velocity and equilibrium data to be dimers in solution (31), and galectin-3 and its truncated version to be predominantly monomers in solution (31), the similarity of  $K_a$  values for galectin-1, -3, and -7 together with truncated galectin-3 and -5 indicates that the observed  $K_a$  values for ASF are independent of the quaternary structures of the galectins. These results are consistent with the inhibitory potency of a monomeric chicken galectin (CG-14) in blocking binding of dimeric galectin-1 to neuroblastoma cells (24). Sedimentation data for galectin-4 and -5 have not been reported. However, galectin-5 is observed to agglutinate rat erythrocytes (32) and rabbit red blood cells (C. F. Brewer and T. K. Dam, unpublished results), suggesting that it may minimally dimerize in the presence of certain carbohydrate ligands. However, it is a monomer as determined by mass spectrometry under conditions that detect homodimers of galectin-1 and -7 (24, 33), and by gel filtration (32).

**$n$  Values for Binding of ASF to Galectin-1, -2, -3, -4, -5, and -7.** Bovine galectin-1 (34) and avian liver galectin-1 (6) have both been reported to bind and precipitate with ASF in solution. The stoichiometry of the precipitation complexes shows a 9:1 galectin:ASF ratio under conditions of excess galectin-1, and the formation of 3:1 galectin–ASF complexes with increasing ASF concentrations. The 9:1 complexes are consistent with binding of all nine LacNAc epitopes of ASF in the respective galectin cross-linked complexes (6, 34).

The ITC-derived  $n$  values of galectin-1, -2, -3, -4, -5, and -7, as well as truncated galectin-3 and -5, show values close to 0.1 (Table 1). We have previously demonstrated that the number of carbohydrate epitopes in a molecule that bind to a lectin is inversely related to the ITC  $n$  values (10). The observed  $n$  values for all of the galectins in Table 1 are consistent with binding of all nine LacNAc epitopes of ASF to the galectins in the ITC experiments.

**$\Delta H$  Values of Binding of ASF to Galectin-1, -2, -3, -4, -5, and -7.** The ITC data for binding of galectin-1, -2, -3, -4, -5, and -7 in Table 1 show  $-\Delta H$  values that are all much greater than the corresponding values for LacNAc, as are the respective  $-T\Delta S$  values. These results are similar to those observed for the binding of di-, tri-, and tetraantennary carbohydrates to ConA and DGL in which the observed  $-\Delta H$  values of the multivalent sugars were much larger than that of the corresponding monovalent analogue (10). In the latter cases, the  $-\Delta H$  values of the multivalent carbohydrates were shown to be roughly proportional to the number of



Table 1: Thermodynamic Parameters for Binding of ASF to Galectin-1, -2, -3, -4, -5, and -7 and Truncated Galectin-3 and -5 at pH 7.2 and 27 °C

	$K_a^a$ ( $\times 10^{-4} \text{ M}^{-1}$ )	$-\Delta G^b$ (kcal/mol)	$-\Delta H^c$ (kcal/mol)	$-T\Delta S^d$ (kcal/mol)	$n^e$
galectin-1 (human)					
ASF	56.0	7.9	43.0	35.1	0.12
LacNAc	1.0	5.5	8.6	3.1	1.00
galectin-2 (human)					
ASF	140.0	8.4	46.0	37.6	0.12
LacNAc	1.9	5.8	9.8	4.0	1.04
galectin-3 (human)					
ASF	140.0	8.4	62.0	53.6	0.11
LacNAc	1.8	5.8	8.9	3.1	1.01
galectin-3 CRD (human)					
ASF	63.0	7.9	52.0	44.1	0.12
LacNAc	1.1	5.5	10.1	4.6	1.03
galectin-4 (human)					
ASF	22.0	7.3	38.0	30.7	0.13
LacNAc	0.35	4.8	9.7	4.9	0.97
galectin-5 (rat)					
ASF	130.0	8.4	61.0	52.6	0.12
LacNAc	1.9	5.8	10.2	4.4	1.04
galectin-5 CRD (rat)					
ASF	190.0	8.6	56.0	47.4	0.11
LacNAc	3.5	6.2	9.3	3.1	0.97
galectin-7 (human)					
ASF	30.0	7.5	44.0	36.5	0.12
LacNAc	0.42	4.9	11.2	6.3	0.98

<sup>a</sup> Errors in  $K_a$  range from 1 to 7%. <sup>b</sup> Errors in  $\Delta G$  are less than 2%. <sup>c</sup> Errors in  $\Delta H$  are 1–4%. <sup>d</sup> Errors in  $T\Delta S$  are 1–7%. <sup>e</sup> Errors in  $n$  are less than 4%.

binding epitopes, with each epitope possessing a  $-\Delta H$  value similar to that of the monovalent epitope. In this case, the observed  $\Delta H$  values for the galectins in Table 1 are less than the sum of the nine LacNAc epitopes of ASF compared to the  $-\Delta H$  value(s) of LacNAc binding to the individual galectins. This may be due to dilution of ASF into solutions of the galectins during the ITC experiments since endothermic heat is associated with control experiments in which ASF is titrated into the buffer, presumably due to ASF binding to itself via carbohydrate–carbohydrate interactions. Hence, the observed  $-\Delta H$  values for the galectins may be lower than expected on the basis of the number of LacNAc epitopes of ASF binding to the galectins.

**Negative Binding Cooperativity of ASF to Galectin-1, -2, -3, -4, -5, and -7.** The Hill plot, in which  $\log(\text{concentration of free ligand})/(\text{fraction of bound protein})/(\text{fraction of free protein})$ , has been used to investigate cooperativity in a variety of ligand–protein systems (cf. 11, 12). Such plots provide evidence for positive or negative cooperativity in the binding of monovalent ligands to multi-subunit proteins. A linear Hill plot with a slope of 1.0 indicates no binding cooperativity. However, Hill plots with slopes of greater than 1.0 indicate positive binding cooperativity, and slopes of less than 1.0 indicate negative binding cooperativity. Thus, the Hill plot has the advantage of assigning numerical values to the degree of cooperativity of the system. The Hill plot also has the advantage of being a logarithmic representation which allows plotting of all obtainable data, unlike double-reciprocal or half-reciprocal plots that often have open upper limits on the abscissa and ordinate (35). Hill plots can also reveal cooperativity associated with binding of multivalent ligands to noncooperative multisubunit proteins such as ConA and DGL (13). In using Hill plot analysis of the binding of a multivalent ligand such as the sugars in this study, the term for the fraction of bound ligand,

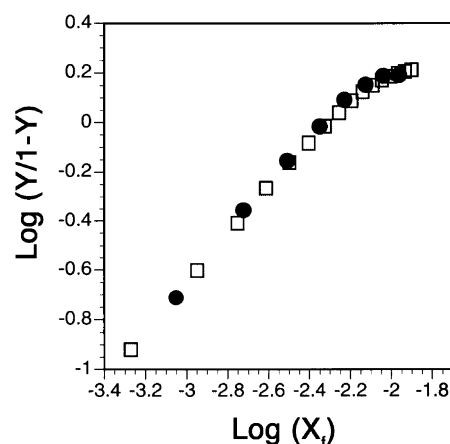


FIGURE 2: Hill plots of ITC data for binding of ASF (330  $\mu\text{M}$ ) to human galectin-3 (34  $\mu\text{M}$ ) (□) and binding of ASF (640  $\mu\text{M}$ ) to truncated galectin-3 (45  $\mu\text{M}$ ) (●). The definition of  $Y$  is given in the text. The functional valency of ASF for the galectins is 9, as determined by ITC.

$X_b/M_t$ , is corrected for the valency of the sugar to give  $X_b \times (\text{functional valency of sugar})/M_t$  which is a modification of the classical Hill plot (see Materials and Methods).

The Hill plots of ITC data for LacNAc binding to galectin-1, -2, -3, -4, -5, and -7 as well as truncated galectin-3 and -5 are essentially straight lines with slopes close to 0.93. This is shown for LacNAc binding to galectin-3 in Figure 5. These slope values are close to a value of 1.0 for noncooperative binding interactions (11, 12), indicating that these galectins do not undergo cooperative binding interactions with this monovalent sugar. Importantly, the absence of allosteric interactions in the galectins upon binding LacNAc allows application of Hill plot analysis to the ITC binding data for binding of ASF to the galectins since the incremental heats measured upon sugar addition and binding are proportional

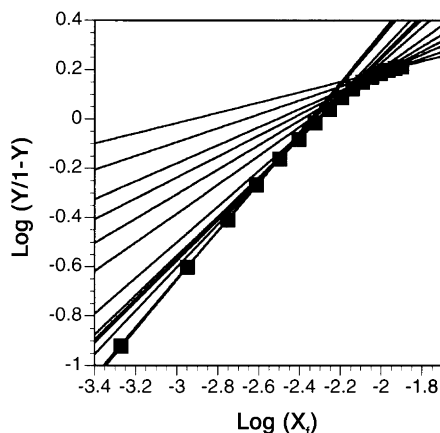


FIGURE 3: Tangent slopes of progressive three-point intervals of the Hill plot for ASF with human galectin-3.

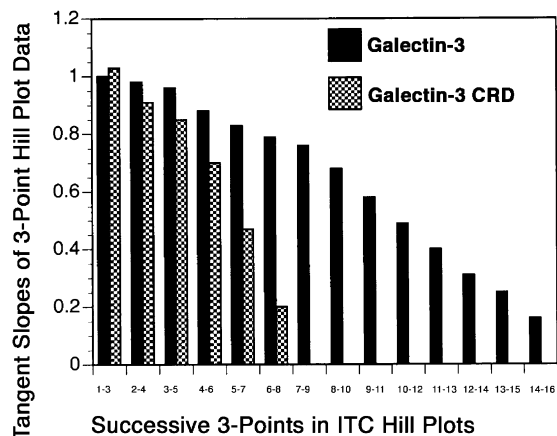


FIGURE 4: Bar graphs of the three-point tangent slopes of the ITC data Hill plots for binding of ASF to galectin-3 and truncated galectin-3.

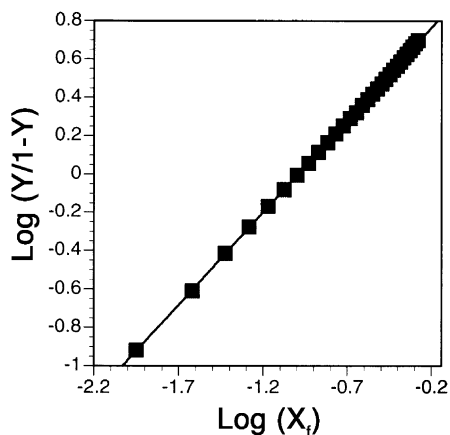


FIGURE 5: Hill plot of the ITC data for binding of LacNAc (7.3 mM) to human galectin-3. The definitions of  $X_f$  and  $Y$  are given in the text. The functional valency of LacNAc is 1, as determined by ITC.

to the number of moles of ligand bound, and not due to allosteric transitions in the lectins. These general conditions are required for Hill plot analysis of ITC data (36).

The Hill plot of the ITC data for binding of ASF to galectin-3 is shown in Figure 2 ( $\square$ ). The plot is curvilinear rather than linear, and disposed around the zero point on the ordinate, as observed for monovalent LacNAc (Figure 5), after correction for the functional valency of ASF. This provides confirmation of the ITC-derived functional valency

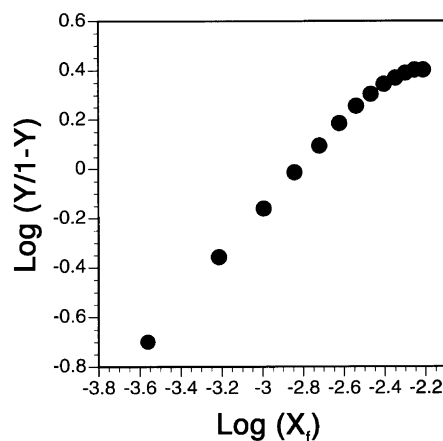


FIGURE 6: Hill plot of ITC data for binding of ASF (395  $\mu$ M) to human galectin-1 (35  $\mu$ M). The definition of  $Y$  is given in the text. The functional valency of ASF for galectin-1 is 9, as determined by ITC.

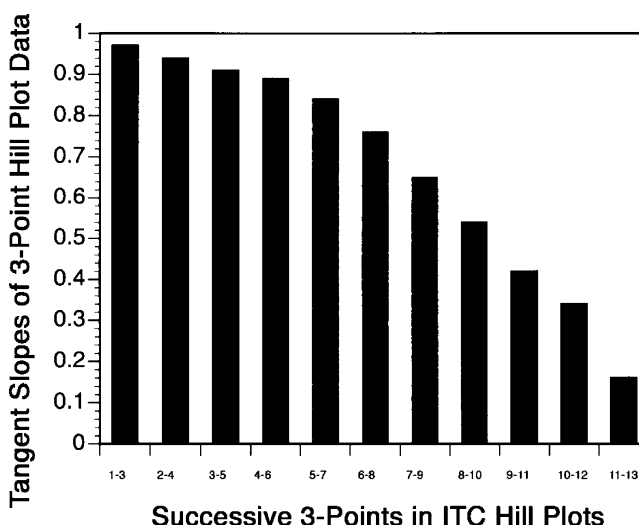


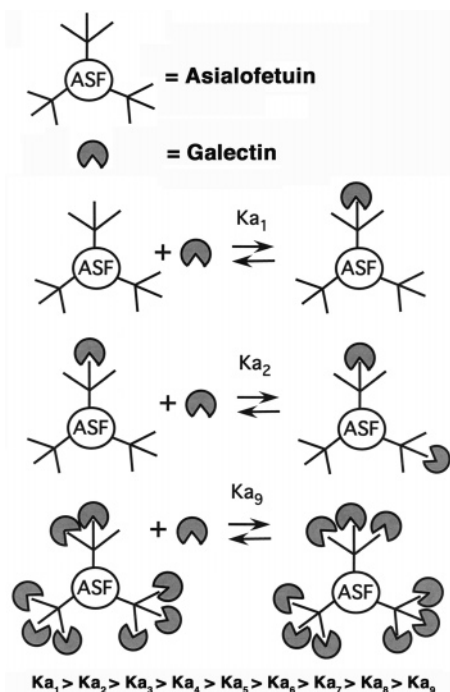
FIGURE 7: Bar graphs of the three-point tangent slopes of the ITC data Hill plots for binding of ASF to human galectin-1.

of ASF for galectin-3. The tangent slopes of progressive three-point intervals of the x-axis of the Hill plot for ASF are shown in Figure 3, which shows decreasing tangent slopes along the binding curve. Figure 4 shows a bar graph comparison of the three-point tangent slopes of ASF binding to galectin-3. The initial tangent slope value is close to 1.0; the final tangent slope value is approximately 0.15. These results show increasing negative cooperativity with increasing binding of ASF to galectin-3.

The Hill plot of the ITC data for ASF binding to truncated galectin-3 is shown in Figure 2 ( $\bullet$ ). The plot is also curvilinear rather than linear, and disposed around the zero point on the ordinate. Figure 4 shows a bar graph comparison of the three-point tangent slopes of ASF binding to truncated galectin-3. The initial tangent slope value is close to 1.0; the final tangent slope value is approximately 0.20. These results show increasing negative cooperativity with progressive binding of ASF to truncated galectin-3.

A Hill plot similar to those for binding of ASF to galectin-3 and truncated galectin-3 was observed for galectin-1 (Figure 6). Figure 7 shows a bar graph of the three-point tangent slopes of ASF binding to galectin-1. Hence, increasing negative cooperativity is observed for the binding

Scheme 1



of ASF to galectin-1. Similar data for ASF binding to galectin-2, -4, -5, and -7 as well as truncated galectin-5 were also observed (not shown). These results indicate that increasing negative cooperativity occurs for binding of ASF to all of the above galectins that represent all three subfamilies of galectins. Furthermore, the negative cooperativity is not due to the quaternary structures of the galectins, since dimeric galectins such as galectin-1, -2, and -7 show similar results as found for monomeric galectins, including galectin-3 and truncated galectin-3 and -5.

**Physical Basis for the Negative Binding Cooperativity in Binding of ASF to the Galectins.** The physical basis of the negative binding cooperativity of ASF to the galectins appears to be similar to that observed for the binding of di-, tri-, and tetraantennary carbohydrates to ConA and DGL (13). Namely, the increasing negative cooperativity observed in the present study is due to the reduction in the functional valency of ASF as it binds an increasing number of galectin molecules. Scheme 1 shows the various microequilibria constants for ASF as it sequentially binds one, two, and up to nine molecules of a galectin. Unbound ASF is functionally nonavalent, with subsequent reductions in its valency with further binding of galectin molecules until the ninth galectin molecule binds to a functionally monovalent ASF molecule. The increasingly curvilinear Hill plots in Figures 2 and 3 for binding of ASF to galectin-3 and its truncated form are consistent with the decreasing functional valency of ASF with progressive binding of galectin molecules. The same is true for binding of ASF to the other galectins.

Another physical factor that was suggested to play a role in the curvilinear Hill plots of di-, tri-, and tetraantennary carbohydrates binding to ConA and DGL (10) was the formation of noncovalent cross-linked complexes between lectin molecules and the carbohydrates. However, the present study shows that ASF possesses essentially the same degree of negative binding cooperativity with truncated galectin-3 and -5 as the full-length molecules (cf. Figures 2 and 6).

Since truncated galectin-3 has been shown to be a monomer in solution by sedimentation velocity experiments (31), and truncated galectin-5 is expected to be a monomer, their negative binding cooperativity with ASF is consistent with the reduction in the functional valency of ASF upon binding of the CRDs of these galectins. Hence, the formation of noncovalent cross-linked complexes between ASF and multisubunit galectins such as galectin-1, -2, and -7 does not appear to significantly contribute to their observed negative binding cooperativity.

**Range of Microscopic  $K_a$  Values for Binding of ASF to the Galectins.** Equation 3 is the general equation derived from our previous studies of the binding of di-, tri-, and tetraivalent carbohydrates to ConA and DGL that relates  $\Delta G(\text{obs})$  to the microscopic  $\Delta G$  values of different epitopes of a multivalent carbohydrate (13).

$$\Delta G(\text{obs}) = (\Delta G_1 + \dots + \Delta G_n)/n \quad (3)$$

Equation 3 states that the observed macroscopic  $\Delta G$  value [ $\Delta G(\text{obs})$ ] of a multivalent carbohydrate binding to a lectin is the average of the microscopic  $\Delta G$  ( $\Delta G_n$ ) values of the individual epitopes, where  $n$  is the number of epitopes. Equation 3 can be written as eq 4 for binding of ASF to the galectins, in which there are nine microscopic  $\Delta G$  values representing the nine microequilibria shown in Scheme 1.

$$\Delta G(\text{obs}) = (\Delta G_1 + \Delta G_2 + \dots + \Delta G_9)/9 \quad (4)$$

The nine microequilibrium constants of ASF are represented by  $K_{a1}$ ,  $K_{a2}$ , ..., and  $K_{a9}$  in Scheme 1, for binding of the first LacNAc epitope of ASF, binding of the second epitope of ASF, and binding of the last unbound LacNAc epitope of ASF to a galectin molecule, respectively. Hence, the observed  $\Delta G$  values [ $\Delta G(\text{obs})$ ] of ASF for the galectins in Table 1 are the average of the nine microscopic  $\Delta G$  terms as shown in eq 4 for each galectin. The relative values of  $\Delta G_1$ ,  $\Delta G_2$ , ..., and  $\Delta G_9$  decrease on the basis of the decreasing microscopic  $\Delta G$  values of the epitopes of multivalent analogues with decreasing functional valencies, as observed for multivalent carbohydrates binding to ConA and DGL (10). In kinetic terms, the microscopic off-rate ( $k_{-1}$ ) for  $K_{a1}$  in Scheme 1 ( $K_{a1} = k_1/k_{-1}$ ) would be expected to be slower than the microscopic off-rate for  $K_{a2}$ , etc., due to binding and recapture of the first bound galectin molecule by the remaining unbound LacNAc residues of ASF before full dissociation of the complex. Since the ITC-derived  $\Delta G(\text{obs})$  value is the average of the nine microscopic  $\Delta G$  values in eq 4, and assuming that there is a symmetrical distribution of decreasing microscopic  $\Delta G$  values on either side of the average  $\Delta G$  value (that is,  $\Delta G_8 - \Delta G_7 \sim \Delta G_3 - \Delta G_2$ , etc.), then the value of  $\Delta G(\text{obs})$  is nearly equal to  $\Delta G_5$  in eq 4. It follows then that if  $\Delta G_9$ , which represents binding of the last free epitope of ASF to a galectin, is nearly equal to  $\Delta G$  for binding of LacNAc to a galectin, then the difference between  $\Delta G(\text{obs})$  and  $\Delta G_9$  is half the difference between  $\Delta G_1$  and  $\Delta G_9$ . Thus, the 2.8 kcal/mol increase in  $\Delta G(\text{obs})$  for ASF binding to galectin-3 versus  $\Delta G$  for LacNAc binding (Table 1) indicates that the difference between  $\Delta G_1$  and  $\Delta G_9$  for binding of ASF to galectin-3 is  $\sim 5.6$  kcal/mol. Since 2.8 kcal/mol is a 78-fold increase in affinity of ASF for galectin-3 over LacNAc, the difference

in affinity of the first unbound LacNAc epitope of ASF for galectin-3 is a  $78 \times 78$  or  $\sim 6000$ -fold increase in affinity over that of LacNAc, with a decreasing gradient of affinities down to that of LacNAc for the last (ninth) unbound epitope of ASF.

Using the same treatment of the data in Table 1, the estimated increase in affinity of the first unbound LacNAc epitope of ASF for truncated galectin-3 versus LacNAc is nearly 3000-fold, demonstrating that the monomeric form of the galectin also shows similar enhanced affinities for the first unbound epitope of ASF. In fact, all of the galectins in Table 1, including truncated galectin-5, show  $K_a(\text{obs})$  values that are 50–78-fold greater than that of LacNAc for the respective galectin. This indicates that the first unbound epitope of ASF binds to all of the galectins with between 3000- and 6000-fold higher affinity than LacNAc and the last unbound epitope of ASF, and therefore, there is a gradient of decreasing affinities for the remaining epitopes of ASF for all of the galectins. In terms of numerical affinity constants, a 6000-fold increase in the affinity of galectin-3 for the first unbound epitope of ASF is equivalent to a  $K_{a1}$  of  $1 \times 10^8 \text{ M}^{-1}$  or a 10 nM affinity constant, using the  $K_a$  value for LacNAc as an estimate for  $K_{a9}$  in Scheme 1. This estimated range of nanomolar affinity constants for  $K_{a1}$  is typical for all of the galectins in Table 1 binding to the first unbound epitope of ASF.

It is important to point out that the above estimates of the range of affinity constants for binding of ASF to the galectins in Table 1 depend, in part, on the assumed affinity of the galectins binding to the last unbound epitope of ASF. In the calculations described above, that affinity constant was estimated to be similar to that of the corresponding monovalent ligand, LacNAc. However, if the affinity of binding of the galectins to the last unbound epitope of ASF is lower than that of LacNAc due to steric crowding or other mechanisms, then the estimated range of enhanced affinity sites on ASF (the first unbound LacNAc epitopes) would be even greater. Likewise, a nonsymmetrical distribution of decreasing binding constants associated with the nine LacNAc epitopes of ASF would also affect the range of estimated affinity constants for the epitopes. Nevertheless, a large range of decreasing affinity constants does exist for the nine epitopes of ASF for the galectins in Table 1, and the estimates for this range in this study are reasonable given the assumptions for such calculations.

*Implications of a Gradient of Decreasing Affinity Constants of ASF for the Galectins.* The implications for a gradient of decreasing affinity constants of ASF for the galectins in Table 1 are important. First, relatively low concentrations of the galectins can be expected to bind to only a few high-affinity sites on glycoprotein receptors such as ASF. In this regard, as few as three galectin-1 molecules bound to ASF have been observed to lead to homogeneous cross-linking of the molecules into large insoluble aggregates (5). This contrasts with the requirement of binding to all of the epitopes of lower-valency molecules such as bi-, tri-, and tetravalent carbohydrates for cross-linking which requires much higher concentrations of lectin to occupy the higher- and lower-affinity epitopes in such molecules (cf. 37). In addition, binding and cross-linking of glycoprotein receptors such as ASF on the surface of a cell by a dimeric galectin such as galectin-1 with individual affinity sites on each

glycoprotein of  $\sim 10 \text{ nM}$  would result in an overall avidity of galectin-1 of  $\sim 10^{16} \text{ M}^{-1}$ . Hence, cross-linking by a dimeric galectin would be essentially irreversible under these conditions.

These observations also apply to other types of lectins interacting with clustered glycan receptors. Fractional high-affinity binding of lectins to multivalent receptors could lead to supramolecular assemblies of homogeneous cross-linked receptors (38) or heterogeneous cross-linked receptors (39). Such assemblies, in turn, can trigger cell surface signal transduction mechanisms similar to those observed for galectin-1 (40).

This study also has general implications for other types of clustered receptor systems. The concept of “spare receptors” is well documented in the pharmacology literature (cf. 41). Maximum dose–activity responses are often observed at relatively low fractional occupancy of the receptors. The present results suggest that such spare receptor systems may exhibit enhanced affinity for a specific ligand through a clustering mechanism similar to that observed for binding of ASF to the galectins in this study. The enhancement in affinity of the ligand could be as much as 1000–10000-fold by clustering of receptors. Occupancy of a portion of the clustered or spare receptors by antagonist would diminish the total number of unbound receptors, but may not reduce the “avidity” of the remaining clustered receptors (41). The “efficacy” of the agonist effect may be related to cross-linking or activating in some manner a fraction of the receptors that is necessary for a full pharmacology effect. In the study presented here, the fractional occupancy by galectin molecules of a few epitopes of an ASF-like receptor molecule could lead to cross-linking interactions and subsequent signal transduction effects such as apoptosis, as observed in the binding of galectin-1 to human T-cell glycoprotein receptors (42).

## REFERENCES

1. Varki, A., Cummings, R., Esko, J., Freeze, H., Hart, G., and Marth, J. (1999) *Essentials of Glycobiology*, p 653, Cold Spring Harbor Laboratory Press, Plainview, NY.
2. Mandal, D. K., and Brewer, C. F. (1993) Differences in the binding affinities of dimeric Concanavalin A (including acetyl and succinyl derivatives) and tetrameric Concanavalin A with large oligomannose-type glycopeptides, *Biochemistry* 32, 5116–5120.
3. Lee, Y. C. (1993) Biochemistry of carbohydrate-protein interaction, *FASEB J.* 6, 3193–3200.
4. Brewer, C. F. (1996) Multivalent lectin-carbohydrate cross-linking interactions, *Chemtracts: Biochem. Mol. Biol.* 6, 165–179.
5. Gupta, D., and Brewer, C. F. (1994) Homogeneous aggregation of the 14-kDa  $\beta$ -galactoside specific vertebrate lectin complex with asialofetuin in mixed systems, *Biochemistry* 33, 5526–5530.
6. Gupta, D., Kaltner, H., Dong, X., Gabius, H.-J., and Brewer, C. F. (1996) Comparative cross-linking activities of lactose-specific plant and animal lectins and a natural lactose-binding immunoglobulin G fraction from human serum with asialofetuin, *Glycobiology* 6, 843–849.
7. Liu, F.-T., Patterson, R. J., and Wang, J. L. (2002) Intracellular functions of galectins, *Biochim. Biophys. Acta* 1572, 263–273.
8. Inohara, H., and Raz, A. (1995) Functional evidence that cell surface galectin-3 mediates homotypic cell adhesion, *Cancer Res.* 55, 3267–3271.
9. Dam, T. K., and Brewer, C. F. (2002) Thermodynamic studies of lectin-carbohydrate interactions by isothermal titration calorimetry, *Chem. Rev.* 102, 387–429.
10. Dam, T. K., Roy, R., Das, S. K., Oscarson, S., and Brewer, C. F. (2000) Binding of multivalent carbohydrates to Concanavalin A and *Dioclea grandiflora* lectin. Thermodynamic analysis of the “Multivalency Effect”, *J. Biol. Chem.* 275, 14223–14230.



11. Stryer, L. (1988) *Biochemistry*, 3rd ed., W. H. Freeman, New York.
12. Di Cera, E. (1995) *Thermodynamic Theory of Site-Specific Binding Processes in Biological Macromolecules*, Cambridge University Press, New York.
13. Dam, T. K., Roy, R., Pagé, D., and Brewer, C. F. (2002) Negative cooperativity associated with binding of multivalent carbohydrates to lectins. Thermodynamic analysis of the "Multivalency Effect", *Biochemistry* 41, 1351–1358.
14. Lahm, H., Andre, S., Hoefflich, S., Kaltner, A., Siebert, H.-C., Sordat, B., von der Lieth, C.-W., Wolf, E., and Gabius, H.-J. (2004) Tumor galectinology: Insights into the complex network of a family of endogenous lectins, *Glycoconjugate J.* 20, 227–238.
15. Leffler, H. (1997) Introduction to galectins, *Trends Glycosci. Glycotechnol.* 9, 9–19.
16. Yang, R.-Y., Hsu, D. K., Yu, L., Ni, J., and Liu, F.-T. (2001) Cell cycle regulation by galectin-12, a new member of the galectin superfamily, *J. Biol. Chem.* 276, 20252–20260.
17. Barondes, S. H., Cooper, D. N. W., Gitt, M. A., and Leffler, H. (1994) Galectins: Structure and function of a large family of animal lectins, *J. Biol. Chem.* 269, 20807–20810.
18. Kasai, K.-i., and Hirabayashi, J. (1996) Galectins: A family of animal lectins that decipher Glycocode, *J. Biochem.* 119, 1–8.
19. Gabius, H.-J. (1997) Animal lectins, *Eur. J. Biochem.* 243, 543–576.
20. Bachhawat-Sikder, K., Thomas, C. J., and Suroli, A. (2001) Thermodynamic analysis of the binding of galactose and poly-*N*-acetylactosamine derivatives to human galectin-3, *FEBS Lett.* 500, 75–79.
21. Ahmad, N., Gabius, H.-J., Kaltner, H., Andre, S., Kuwahara, I., Liu, F.-T., Oscarson, S., Norberg, T., and Brewer, C. F. (2002) Thermodynamic binding studies of cell surface carbohydrate epitopes to galectin-1, -3, and -7. Evidence for differential binding specificities, *Can. J. Chem.* 80, 1096–1104.
22. Gabius, H.-J. (1990) Influence of type of linkage and spacer on the interaction of  $\beta$ -galactoside-binding proteins with immobilized affinity ligands, *Anal. Biochem.* 189, 91–94.
23. Sturm, A., Lensch, M., Andre, S., Kaltner, H., Wiedenmann, B., Rosewicz, S., Dignass, A. U., and Gabius, H.-J. (2004) Human galectin-2: Novel inducer of T cell apoptosis with distinct profile of caspase activation, *J. Immunol.* 173, 3825–3837.
24. Andre, S., Kaltner, H., Lensch, M., Russwurm, R., Siebert, H. C., Fallsehr, C., Tajkhorshid, E., Heck, A. J. R., von Knebel-Doberitz, M., Gabius, H.-J., and Kopitz, J. (2005) Determination of structural and functional overlap/divergence of five proto-type galectins by analysis of the growth-regulatory interaction with ganglioside GM1 *in silico* and *in vitro* on human neuroblastoma cells, *Int. J. Cancer* 114, 46–57.
25. Andre, S., Kaltner, H., Furuie, T., Nishimura, S., and Gabius, H.-J. (2004) Persubstituted cyclodextrin-based glycoclusters as inhibitors of protein-carbohydrate recognition using purified plant and mammalian lectins and wild-type and lectin-gene-transfected tumor cells as targets, *Bioconjugate Chem.* 15, 87–98.
26. Ahmad, N., Gabius, H.-J., Sabesan, S., Oscarson, S., and Brewer, C. F. (2004) Thermodynamic binding studies of bivalent oligosaccharides to galectin-1, galectin-3, and the carbohydrate recognition domain of galectin-3, *Glycobiology* 14, 817–825.
27. Dubois, M., Gilles, K. A., Hamilton, J. K., Rebers, P. A., and Smith, F. (1956) Colorimetric method for determination of sugars and related substances, *Anal. Chem.* 28, 350–356.
28. Saha, S. K., and Brewer, C. F. (1994) Determination of the concentrations of oligosaccharides, complex type carbohydrates and glycoproteins using the phenol-sulfuric acid method, *Carbohydr. Res.* 254, 157–167.
29. Wiseman, T., Williston, S., Brandt, J. F., and Lin, L.-N. (1989) Rapid measurement of binding constants and heats of binding using a new titration calorimeter, *Anal. Biochem.* 179, 131–137.
30. Brewer, C. F. (2002) Binding and cross-linking properties of galectins, *Biochim. Biophys. Acta* 1572, 255–262.
31. Morris, S., Ahmad, N., Andre, S., Kaltner, H., Gabius, H.-J., Brenowitz, M., and Brewer, C. F. (2004) Quaternary solution structures of galectins-1, -3 and -7, *Glycobiology* 14, 293–300.
32. Gitt, M. A., Wiser, M. F., Leffler, H., Herrmann, J., Xia, Y.-R., Massa, S. M., Cooper, D. N. W., Lusi, A. J., and Barondes, S. H. (1995) Sequence and mapping of galectin-5, a  $\beta$ -galactoside-binding lectin, found in rat erythrocytes, *J. Biol. Chem.* 270, 5032–5038.
33. Kopitz, J., Andre, S., von Reitzenstein, C., Versluis, K., Kaltner, H., Pieters, R. J., Wasano, K., Kuwabara, I., Liu, F.-T., Cantz, M., Heck, A. J. R., and Gabius, H.-J. (2003) Homodimeric galectin-7 (p53-induced gene 1) is a negative growth regulator for human neuroblastoma cells, *Oncogene* 22, 6277–6288.
34. Mandal, D. K., and Brewer, C. F. (1992) Cross-linking activity of the 14-kilodalton  $\beta$ -galactose-specific vertebrate lectin with asialofetuin: Comparison with several galactose-specific plant lectins, *Biochemistry* 31, 8465–8472.
35. Weber, G., and Anderson, S. (1965) Multiplicity of binding. Range of validity and practical test of Adair's equation, *Biochemistry* 4, 1942–1947.
36. Indyk, L., and Fisher, H. F. (1998) Theoretical aspects of isothermal titration calorimetry, *Methods Enzymol.* 295, 350–364.
37. Dam, T. K., Roy, R., Pagé, D., and Brewer, C. F. (2002) Thermodynamic binding parameters of individual epitopes of multivalent carbohydrates to Concanavalin A as determined by "reverse" isothermal titration microcalorimetry, *Biochemistry* 41, 1359–1363.
38. Brewer, C. F. (1997) Cross-linking activities of galectins and other multivalent lectins, *Trends Glycosci. Glycotechnol.* 9, 155–165.
39. Ahmad, N., Gabius, H.-J., André, S., Kaltner, H., Sabesan, S., Roy, R., Liu, B., Macaluso, F., and Brewer, C. F. (2004) Galectin-3 precipitates as a pentamer with synthetic multivalent carbohydrates and forms heterogeneous cross-linked complexes, *J. Biol. Chem.* 279, 10841–10847.
40. Brewer, C. F., Miceli, M. C., and Baum, L. G. (2002) Clusters, bundles, arrays and lattices: Novel mechanisms for lectin-saccharide-mediated cellular interactions, *Curr. Opin. Struct. Biol.* 12, 616–623.
41. Goldstein, A., Aronow, L., and Kalman, S. M. (1974) *Principles of Drug Design*, 2nd ed., pp 101–104, John Wiley & Sons, New York.
42. Pace, K. E., Lee, C., Stewart, P. L., and Baum, L. G. (1999) Restricted receptor segregation into membrane microdomains occurs on human T cells during apoptosis induced by galectin-1, *J. Immunol.* 163, 3801–3811.

BI051144Z